THE HELIUM ATOM MICROSCOPE - REPORT ; 1

(1/10/91 - 1/3/92)

J. Lower

Table of Contents

Abstract

In this first report I assess the feasibility of developing a high resolution surface sensitive microscope which uses helium atoms as it's imaging medium. That it is possible to build an imaging atom microscope is not in question. However, when one asserts that without a very high resolution (i.e. ≤ 1000 Å) such a microscope would likely provide no superior alternative to optical and electron microscopes presently in use, then the task is rendered considerably more difficult. My aim has been to establish an optimum development plan through the identification and clarification of problems which, to date, have obstructed the realization of such a device. The perspective presented in this report is the result of five months research in the Max Planck Institut für Strömungsforschung, Göttingen.

I present in Chapter I a number of simple geometries which an atom microscope could assume and discuss the limitations concomitant to each. It is concluded that a configuration in which both the primary atom beam and atoms scattered from the target undergo focussing provides the best opportunity to achieve both high count rate and high resolution.

Rather than embarking upon a general review of atom detectors common to usual atom scattering studies, I concentrate in Chapter II upon the field ionization detector, a detector possessing both a high spatial resolution and a high detection efficiency. I then illustrate a scheme by which a resolution substantially smaller than the ionization area of such a device might concievably be achieved, whereby significant gains in resolution are wrought without concomitant reductions in collection efficiency.

Chapter III constitutes a critical appraisal of both the "atomic mirror" and the Fresnel zone plate as possible atom focussing elements for eventual incorporation into a rudimentary atom microscope. To start, I show the extreme sensitivity of the focussing

3

properties of the atomic mirror on both macroscopic and microscopic shape imperfections. I do this through a calculation of the aberrations resulting from spherical and parabolic approximations to the ideal elliptical form and by calculating the resolution degrading effects of mosaic structure present on the mirror surface. A method of crystal bending. based upon the electrostatic force between two metal plates. is presented as an alternative to the usual mechanical methods with the promise of improved accuracy. Finally. it is concluded that while the atomic mirror can play a significant role as a means to intensify the primary beam in an atom microscope. it probably cannot be formed to sufficient accuracy to image a surface with high resolution. The discussion then turns to the Fresnel zone plate. After a short review of theory. it is concluded that with a commercially available zone plate. resolutions of $\leq$ 1000 Å could conceivably be achieved by using a higher order diffraction image in conjunction with a "point like" field ionization detector. if the illuminated target area can be made sufficiently small.

Irrespective of count rate or resolution level achieved. an image of a surface with no contrast provides no information. In Chapter IV the concepts of image contrast are developed through some simple examples. It is shown that "spatial filtering" of diffracted atoms. before processing by the imaging lens. may not be available as a means to improve contrast due to finite source size and mosaic spread of the target surface. A realistic estimate of the expected count rate from a microscope based around a Fresnel lens is made and a technique by which significantly improved count rate. for the specific case of isolated defects on an otherwise perfect crystal surface. is presented. It is concluded that for general imaging of target surfaces. substantial focussing of the incident beam will be required to bring count rate to an acceptable level.

Finally. Chapter V provides an assessment of the progress to date and proposes the next development stage towards the realization of a helium atom microscope.

I. Fundamentals of Microscope Design

I wish to start with a very general discussion of possible microscope geometries employing atom focussing elements. Broadly speaking. the design would fall into either of the following two categories (i) One in which an incident atom beam is focussed onto a small spot on the target. the size of the spot determining the resolution of the microscope. The target surface is scanned by either sweeping the incident beam across the sample or by moving the target itself. (ii) One in which the target is illuminated by a broad incident beam. Scattered particles leaving a small region of the target surface. the size of which is determined by the imaging lens. being focussed onto a detector. An image over an extended area of surface is achieved by scanning the detector across the lens image plane or again by moving the target in small steps. The two schemes are illustrated schematically below and their relative merits assessed in turn.
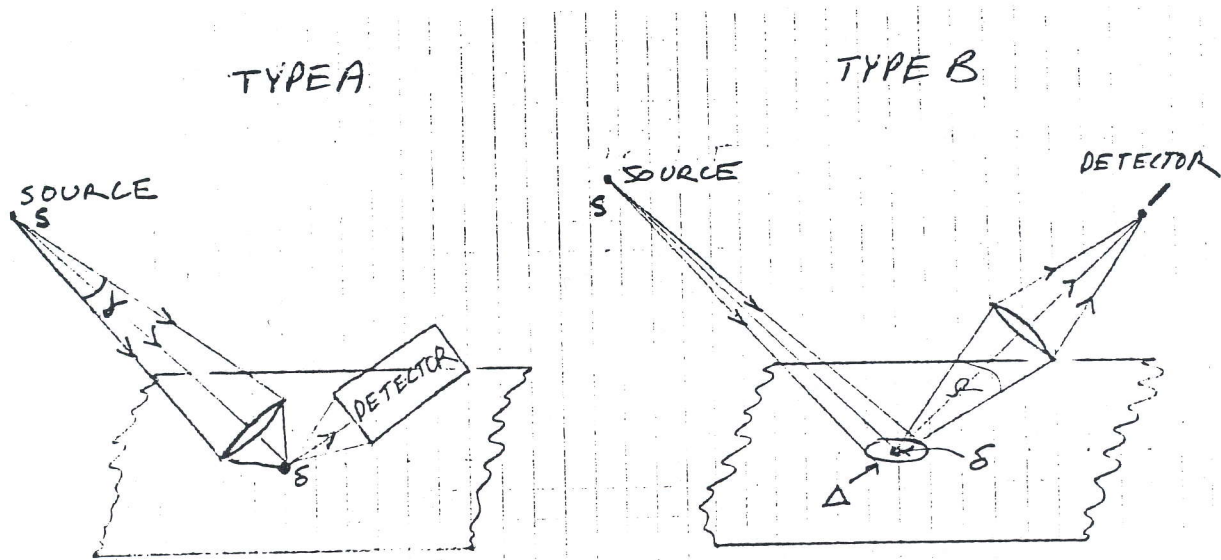

Figure I.1

The ultimate resolution of the type A microscope is ultimately limited by the source size s. In the limit of an ideal beam focussing element. a spot size $\delta = s/k$ can be

achieved simply through demagnification of the source by a factor k. For atomic focussing applications however, this avenue appears most difficult, due to the intrinsically long focal length f of atoms mirrors or zone plates presently being considered as possible candidates for microscope focussing elements. Very roughly, the required distance between source and target scales with the magnification M when M is large. Furthermore, on the basis of measurements by Doak [1] it is not clear whether the source size might not generally be many times larger than the aperture dimension d for nozzle sources of the type generally employed in helium scattering experiments. Doak points out that although, in theory, the source size s at the " sudden freeze " surface scales with the nozzle diameter d by the relation $s = d \rightarrow d^{1.5}$ (Excluding, of course, the effect of collimating apertures further down stream, whose geometry will also influence the source size), the measured source size for the 10 μ nozzle used in his experiments was 500 μ ! Athough unable to give a satisfactory explanation to this anomolous result, he points out that to date helium beam sources have been optimised to minimize the velocity spread in the direction parallel to the beam direction, essentially ignoring the spread in the perpendicular direction. He suggests that the source size s could be reduced through tailoring the flow characteristics of the nozzle, rather than by reducing the nozzle diameter d or source pressure, both of which would have detrimental effects on count rate. It will be shown later (Section IV) that a small source size and beam convergence angle can also be important for good image contrast, depending upon the angular distribution of scattered atoms from the target surface.

In the type B Microscope the target surface is quasi-uniformly illuminated over an area Δ much larger than the sampled area δ from which scattered particles are collected. The imaging lens focusses particles from δ onto a point at the detector plane. The final resolution is determined by both the resolution of the focussing element and that of the detector, in contrast to the type A microscope, where the detector resolution plays no role. The ultimate resolution is independent of the source size in this case. The greatest

6

drawback of this method is its intrinsic inefficiency (assuming one cannot put an extended area position sensitive detector in the lens focal plane and simultaneously collect signal from an extended area of surface whilst still maintaining good spatial resolution). Namely, that the area δ from which scattered particles are collected is in general much smaller than the total illuminated area Δ. Thus assuming uniform illumination of the surface, contributions from only $\frac{\delta}{\Delta} \times$ 100 % of the surface are being collected at any time - the remaining $(1 - \frac{\delta}{\Delta}) \times$ 100 % only serving to increase the background gas pressure and consequently background count rates, perhaps even to an extent where the true signal is swamped by background signal. For example, with a resolution of spatial resolution of 0.1μ and a incident beam spot size of 1 mm, scattered particles eminating from only 10^{-6} % of the illuminated surface area are being observed at any given time. The beam intensity incident upon δ for a given nozzle pressure can be many orders of magnitude lower than in the type A microscope, where the incident flux is concentrated through the agency of the primary beam focussing element. On the other hand, the small range of angles incident upon δ is conducive to image contrast enhancement techniques as shall be shown in Section IV.

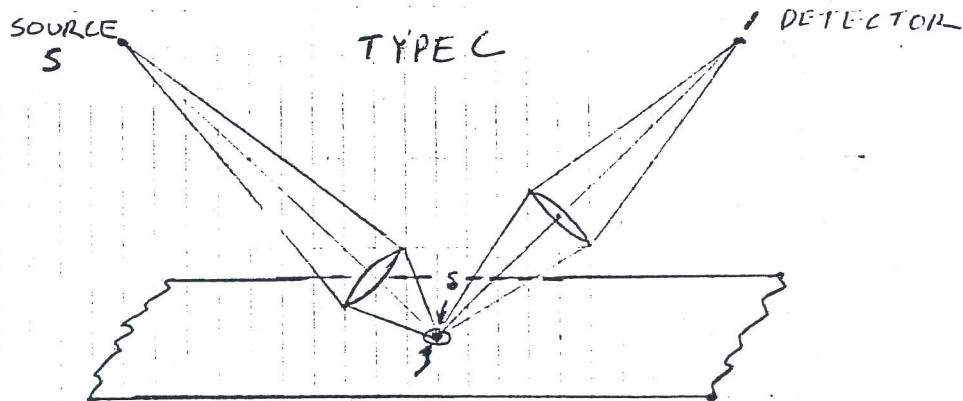

Figure I.2

The question then arises if one could not design a microscope where the incident beam is focussed onto a small surface spot of area ζ solely as a means to improve beam

intensity, but the resolution constraint imposed by the finite source size s is removed by imaging the much smaller area c area through a second focussing element, which itself then determines the resolution of the microscope. This hybrid of types A and B will be termed a type C microscope in future discussions and is illustrated above.

In summary, the type A microscope is the most efficient design from the point of view of high countrate and low background signal levels if one can develop an analyser to detect atoms over a large scattering solid angle and with a reasonable detection efficiency. It's ultimate resolution, however, is restricted by the source size s although the spatial resolution of the detector plays no role here. The ultimate resolution of types B and C depends only upon the quality of the imaging lens <u>and</u> that of the detector employed. Type B suffers in count rate due to a relatively low incident beam intensity. Microscope C provides a partial solution to this problem, but perhaps at the expense of decreasing image contrast through focussing of the incident beam. Which particular configuration would prove most effective in any given application will be determined by the quality of the available atom sources, lenses and detectors.

II. Atom Detectors

Microscopes B and C require a detector of good spatial resolution. For this purpose the field ionization detector (FID) presents itself as an ideal candidate. It's characteristics include a spatial resolution R_d of less than 1000 Angstroms determined by the tip radius r and a detection efficiency of close to 1.0. A detailed description of it's operating principles can be found in reference [2]. I note in passing that it <u>may</u> be possible, through optimization of the tip voltage, size, composition etc. to achieve a spatial resolution smaller than the tip ionization area for such a detector, thus achieving parallel detection to some limited degree and hence improved collection efficiency. I have not yet had time to investigate this possibility in detail but the idea is as follows (see diagram below).

8

If the multiple collisions an incoming helium atom makes with the surface before ionization are localized to a small neighbourhood δ_{imp} of its initial impact coordinate, then the arrival coordinate of the resultant ion on a distant position sensitive detector can be used to deduce the initial impact coordinate of the atom to an accuracy of approximately δ_{imp} i.e. smaller than the active ionization area of the tip itself.

Note that all trajectories of incoming atoms (each of which is specified by an impact parameter b_i) are essentially parallel to one another before they come under the influence of the high field strength near the tip. It follows that any small deviations in trajectory they later experience, as they proceed closer to the tip surface, should not affect the above arguments. as atoms of each impact parameter b_i are mapped into a unique angular coordinate θ_i in the limit $\delta_{imp} \rightarrow 0$. the potential at the tip having approximately spherical symmetry.
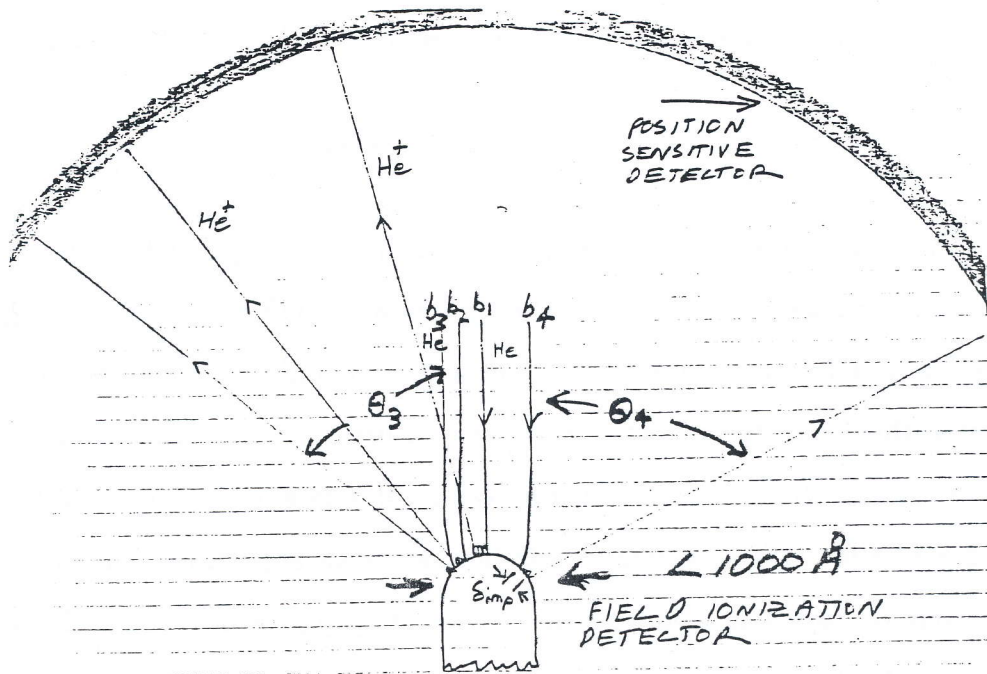

Figure II.1

III. Atom Beam Focussing

III.1   Introduction

Two possible means of atom focussing will be considered in this section, namely, through their reflection from the surface of an atomic mirror or by their diffraction through the agency of a transmission Fresnel zone plate. The relative merits of these two approaches will be assessed in turn. I have not yet investigated the possibility of atom focussing by the agency of strong electromagnetic fields and must therefore leave a relevant discussion to a later date. First I consider the possibility of using an atomic mirror to focus atoms. I show that the form of the focussing mirror must approximate it's ideal elliptical form to an extreme degree of accuracy, on both microscopic and macroscopic scales, if a resolution $\leq$ 1000 $\mathring{A}$ is to be achieved. This is done by calculating the aberrations introduced through approximating the ideal elliptical mirror by spherical and parabolic forms and by calculating the adverse effect of surface mosaic spread on it's focussing ability.

III.2   Mirror Aberrations

Only the ellipsoidal focussing mirror achieves true point to point focussing between object and image points lying on the optical axis. Off axis focussing, even for a perfect ellipse, is not free from aberrations. However, scanning surface structure by moving the target rather than the detector in an atom microscope incorporating a "point like" field ionization detector avoids the introduction off-axis aberrations completely. This option being available, it is sufficient to ask how good an approximation to the elliptical shape is a circle or parabola from the view point of on axis aberrations. Note that the ideally required elliptical shape may not be accesible in any given type of mirror fabrication technique i.e. bending of a crystal under the action of an applied force. For example, calculations of the deflection undergone by a circular plate under the action of a uniform gravitational field [9], for the cases of both free and clamped edges, show the plate assumes

10

forms other than the elliptical forms considered above. Furthermore. it is not always made clear in engineering handbooks etc. whether or not the deformation formulae presented are exact or the result of approximations. Such a question is of little consequence for general design considerations but critical to those for the production of an atomic mirror. due to the stringent shape requirements imposed.

Let us begin with some fundamentals. A circle is the limiting case of an ellipse when the two focii are infinitely close together. The parabola. on the other hand, is the limiting case when one focus is at infinity. The relative focussing performance of the ideal elliptical mirror with it's corresponding circular and parabolic approximations will now be compared. Consider the diagram below.
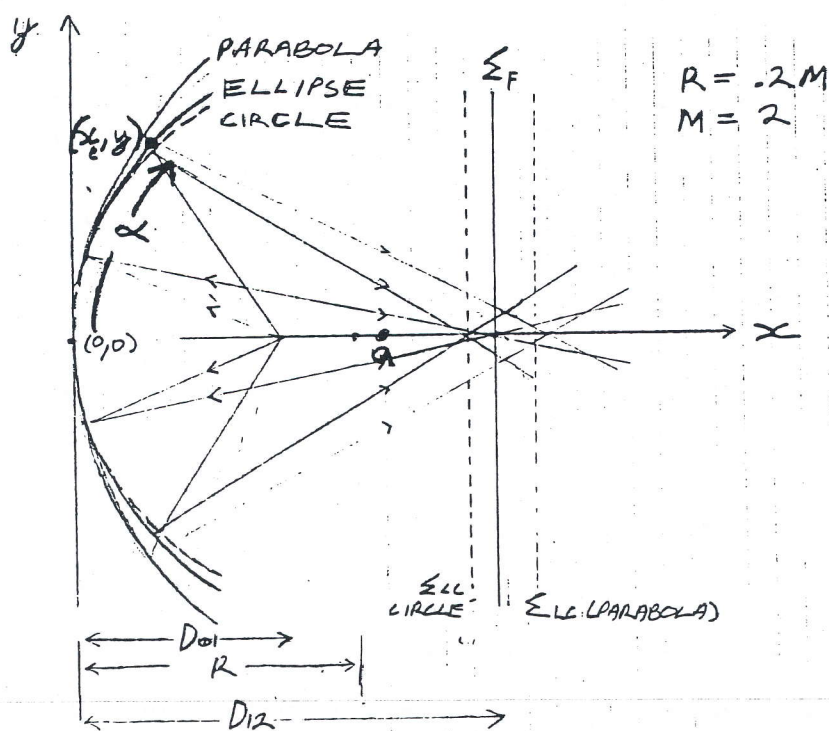

Figure III.1

The target (object) is at a distance D_{01} and the image (detector) at a distance D_{12} from the surface of a focussing mirror. The following parameters: $D_{01} = .3$ m and $D_{12} = .6$ m have been chosen as realistic length scales on two grounds. The first. due to the

expected worsening defect structure of a crystal mirror as the mirror radius of curvature is reduced. The second, to allow sufficient distance between the two focii in order to reduce the size of "shadow" cast on the mirror surface by an object placed at the first focus as seen at the second. The magnification $M = \frac{D_{12}}{D_{01}} = \times 2$ in this case. The reader is referred to Appendix 1 for the derivation of the relevant aberration formulae, the values of which, for the present parameters, are displayed in the table below. Included for interest is a comparison with the diffraction limited resolution $\delta_{Rayleigh}$ corresponding to mirrors of different sizes. The Rayleigh criterion [5] states that the minimum spatial resolution $\delta_{Rayleigh}$ in the target which can be resolved with a wavelength λ due to diffraction limitation is given by the formula:

$$\delta_{Rayleigh} = \frac{0.61\,\lambda}{\sin\alpha} = \text{(in this example)} \; \frac{0.61\,\lambda\,D_{01}}{y} . \qquad (III.13)$$

α being the semi-angle subtended by the object at the focussing element as shown in Figure III.1. λ was chosen to be 1.0 $\overset{\circ}{A}$ for the sake of illustration.

The symbol definitions are as follows. y represents the lateral distance across the mirror surface, x_ϵ the height of the ellipse at any arbitrary point y. $x_{c\epsilon}$ and $x_{p\epsilon}$ respectively the difference in height between the circle and the parabola from the ideal elliptical form. δy_c and δy_p are the respective errors (abberations) in arrival position of reflected atoms at the focal plane Σ_F of the ellipse. $\delta_{Rayleigh}$ is the diffraction limited resolution for a mirror of radius y. The values δy_c and δy_p as recorded in the table below have been corrected (division by 3) to allow for the opportunity of positioning a detector at the " plane of least confusion " Σ_{LC} [7], whereby the adverse effects of aberration can be reduced to some extent. In the diagram below this correction procedure is illustrated in a little more detail for a circular mirror of radius .2 m (not .4 as in the present example) and for a magnification again of 2.0.
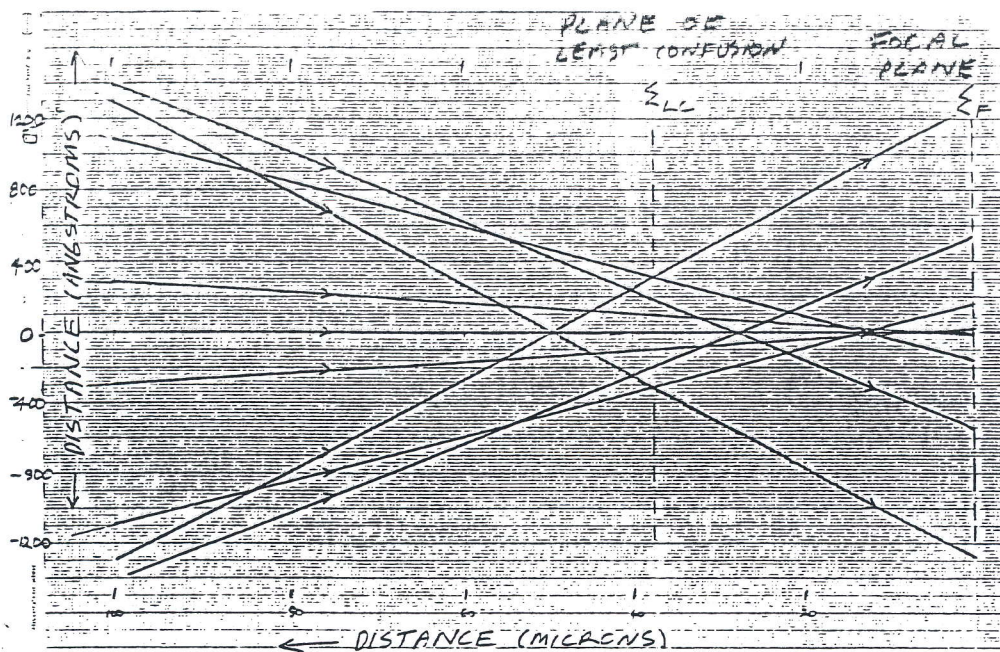
12

Figure III.2

Table III.1   Mirror aberrations

y	x_ϵ	$x_{c\epsilon}$	$x'_{p\epsilon}$	δy_{c} (corr.)	δy_{p} (corr.)	$\delta_{Rayleigh}$
mm	μ	$\overset{\circ}{A}$	$\overset{\circ}{A}$	$\overset{\circ}{A}$	$\overset{\circ}{A}$	$\overset{\circ}{A}$
1	1.3	.002	-.017	1.7	14	183
2	5.0	.035	-.28	14	111	92
3	11.3	.176	-1.4	47	376	61
4	20	.556	-4.4	111	900	46
5	31	1.36	-10.9	216	1733	37
10	125	21.7	-174	1733	$1.4\ \mu$	18

Note from the above results how the small, smoothly increasing height differences between the ideal ellipsoidal and the circular and parabolic mirrors which approximate it (x_{ce} and y_{pe} respectively), project into large aberrations at the detector plane Σ_{LC} due to the macroscopically large distance D_{12} separating mirror and focal plane e.g. the results show that a height difference of only 10.9 $\mathring{A}$ between the parabolic and the ellipsoidal mirror at a distance of 5 mm across the mirror surface translates into an aberration in the arrival position of a reflected atom of 0.17 μ at the plane of the detector Σ_{LC} ! This simple illustrations shows how extreme is the required degree of perfection in the macroscopic mirror form if high resolution is demanded.

The physical size of a focussing mirror is thus chosen by balancing the conflicting requirements of high collection capability and diffraction limited resolution with the increasing difficulty of producing an accurate form over large macroscopic areas. Having decided upon mirror dimensions, an appropriate production technique must be chosen. Two possible methods will be considered in this report. The first, to take a crystal whose surface exhibits a high degree of perfection on the microscopic scale and attempt to bend it into the correct macroscopic form. The second, to utilize a commercially available ground glass substrate, whose macroscopic ellipsoidal form is highly accurate when observed with a lateral resolution $\geq 1\mu$ and through the deposition of surface layers, hope to smooth out atomic scale irregularities. The quality of mirror achieved by either method will depend critically upon the extent to which the surface is free from mosaic spread as will now be demonstrated.

III.3 Defects on the Microscopic Scale

A mosaic crystal is one in which the ideal lattice regularity is restricted to very small regions of the surface. the boundaries of which are fixed by distortions and displacements. From the perspective of a mirror surface. a problem arises because each of the small facets has a slightly different angle of orientation with respect to its neighbour. each differing in orientation by an amount $\delta\theta$ from the perfect elliptical surface to which they should confirm. If the facets are many angstroms across. each can be considered as a small mirror to an incoming helium atom. Consider the simple one dimensional model drawn below where. for the sake of argument. the facets have been given an average spread in orientation of 2×10^{-6} radians (10^{-4} °). Inter-facet interference effects will be ignored in this simple model. but their inclusion should not affect the picture greatly if each facet is many thousand angstroms in extent.
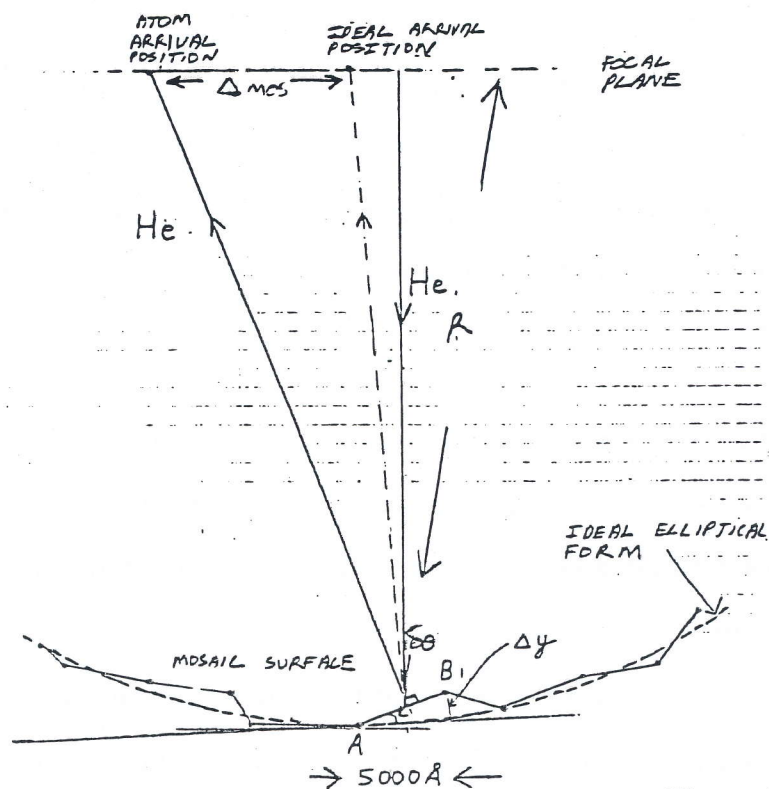

Figure III.3

15

In such a case, any deviation in facit orientation $\delta\theta$ from that ideally required translates directly into a resolution degrading uncertainty Δ_{mos} at the image plane a distance R away, where $\Delta_{mos} \simeq R\delta\theta$. For example, for $R = .5$ m, a realistic focal length for an atom focussing element, and $\delta\theta = 2 \times 10^{-6}$ radians (10^{-4} °), then $\Delta_{mos} = 1\mu$. More dramatically for the case of mica, where $\delta\theta$ is quoted at 10^{-1} ° [1], $\Delta_{mos} = 1$ mm !!! Other measurements from gold grown epitaxially on mica [3] show the mosaic spread of the resultant crystallites to be of considerably larger value than the mica substrate itself !

There is even a more disturbing ramification of the mosaic effect which can be seen from the above diagram, namely, that tiny changes in orientation $\delta\theta$ across the crystal surface may well be undetectable by standard surface analysis techniques. Consider the facet of length 5000 Å bounded by the points A and B. Due to the 2×10^{-6} radian deviation in normal direction, the point B is a height $\Delta y = 5000 \times 10^{-6} = 5 \times 10^{-3}$ Å too high from the ideal elliptical surface to which it should conform. Even an STM would not be able to detect such a height difference ! - and remembering, it was shown above that an average spread $\delta\theta$ of 2×10^{-6} corresponds to an ultimate resolution of 1μ, much worse than we would ultimately hope to achieve in a microscope. For a possible resolution of 500 Å the average height variation tolerable across similarly dimensioned facets would be only 2.5×10^{-4} Å.

Whether mosaic spread, as I have interpreted it, is present to some degree in all crystal surfaces or not, I do not know. Doak [1] attributed his lack of success at obtaining a focus of better than a factor of four to the 0.1° mosaic structure of his mica sample, finally ruling out mica as a candidate for a high resolution atom focussing mirror. Furthermore, I have not yet researched the effect of bending on mosaic surface structure, which indeed might worsen the situation ! Therefore, of fundamental importance to the development of a high precision atomic mirror is to first establish the constraints which exist, be they determined on theoretical or technological grounds, which in any way limit the degree to

16

which a surface can be free of mosaic spread. Such an investigation probably presents the fastest route to developing a high quality mirror surface, as crystal bending techniques can forever be refined. Such an investigation may indeed show that a surface of the required perfection is ruled out on purely theoretical grounds.

Consider now a few other surface imperfections which might, through their presence, degrade the performance of an atomic mirror. Step edges, contaminant atoms and other localized imperfections, if in low concentration, will not affect mirror performance to any significant degree, serving only to remove atom current from the diffracted beams through diffuse scattering. The presence of islands on the crystal surface also can be neglected if their concentration is low and the incident wavelength matched so that an integer number of wavelengths is equal to the height of a mono-atomic step. If the wavelength is not matched to the step height, then each island acts as an incoherent emitter with respect to all others and the effective diffraction limited resolution is determined by the average island size.

III.4   Crystal Bending Techniques

To form an elliptical mirror from a crystal. one needs to develop a highly accurate bending method. Mechanical methods for crystal bending have been well developed for X-ray and neutron beam focussing applications. however in these cases. the required bending accuracy is orders of magnitude less than is required to produce a high resolution micro-scope lens. As a possible alternative to the use of mechanical force with the possibility of improved accuracy. I shall consider here a method based upon the electrostatic attraction between two metal plates. each of different potential.

The idea is to use a commercially produced elliptical glass mirror. whose shape accuracy is extreme when observed with a spatial resolution of > 100 Å, as a substrate into which a thin crystal sheet can be accurately pressed using electrostatic force. This would be achieved in the following fashion. Firstly. one would coat the mirror surface with a few layers of metal to form a conducting surface layer. The selected crystal sheet, if insulating (e.g. mica). would have its front face also coated with a few metal layers in order to form a second conducting surface. An applied potential difference between the two surfaces then provides the necessary force. Such a technique has a number of advantages over the mechanical bending techniques. where the applied force is concentrated around the periphery of the crystal plate. Firstly. the electrostatic force is completely uniform and its direction always at a normal to the elliptical surface as is ideally required. Secondly. the edges of the crystal are free. in contrast to the case with mechanical bending devices. allowing a better opportunity to relieve bending induced internal stress. Finally. the crystal is supported at all points over it's surface. greatly reducing sensitivity to vibration.

Consider the case of a 1 cm^2 circular piece of mica. thickness 0.1 mm (admittedly. mica has a remarkably high 150 Kv/mm breakdown potential and is. to this extent. a

18

rather exceptional case). The force F between two plates of cross-sectional area A, separated by a medium of dielectric constant κ, a distance d apart and possessing a difference in potential of V volts is given by the following:

$$F = .5\left(\frac{V}{d}\right)^2 A \kappa \epsilon_0$$

$$= .5\ (1.5 \times 10^8)^2\ (1 \times 10^{-4}) \times 5.4 \times 8.85 \times 10^{-12}$$

$$= 53\ \text{Nt} \simeq 5.4\ \text{Kg maximum} \qquad\qquad (III.14)$$

Other insulating materials do not have anywhere near so high a breakdown potential, however this example illustrates that reasonable pressures can concievably be achieved with this method. In the case where a semi-conducting or conducting crystal surface is to be employed, a thin sheet of mica could be inserted as an insulating layer between the crystal and the mirror substrate (in the case of a semiconductor, coating its backside with a fine metal layer), again utilizing the extreme capacitive force available with mica and the fact that it cleaves along crystal planes to form a sheet of remarkably constant thickness. Perhaps a few mono-layers of oil introduced between the layers might also assist the technique. Although I believe that these methods should work well, I doubt whether sub-micron resolutions could be achieved in this fashion.

A second possibility to produce a high quality atom mirror is take one of the commercially available elliptical mirrors, referred to above and deposit upon it's surface metal layers, in an attempt to smooth out roughness on the atomic scale. Through various heating cycles, it would be hoped to form a surface comprising of small atomically smooth regions, whose orientations conform accurately to those ideally required. How feasible this method would be must be determined experimentally, although on the basis of what I have read so far, the chances of forming an atomically smooth surface in this way of quality sufficient for a microscope imaging lens, seem remote. For example, considerable work has

19

been done on the growth of gold on a mica. In the comprehensive work of Chidley *et al* [3] they found that under best experimental conditions they were able to form islands of 4000 Å diameter. however the deposited gold surface possessed a mosaic spread of 0.4° i.e. four times worse than the mica substrate itself ! Even if a surface of well orientated crystalites could be formed. whether the individual crystalite surfaces themselves would assume the correct elliptical curvature or in fact be planar is indeed not clear. As pointed out by Doak [1]. a piecewise approximation to the focussing surface will only be able to focus down to a spot size comperable to the "piece size" itself.

III.5   Techniques for Beam Enhancement

The development of atomic mirrors for use as beam focussing elements is in itself an extemely important goal. irrespestive of whether the requisite precision for a microscope lens can be reached. For such applications. the required mirror accuracy is <u>many</u> orders of magnitude less than would be required for a microscope lens i.e. a mirror focussing capability of a millimeter over a half meter focal length might. in a given application. be entirely sufficient. Doak [1] points out that a possible $> 10^5$ increase in incident beam current could concievably be obtained through purely steric effects using an atom mirror to concentrate the flux from a nozzle source.

Figure III.4

20
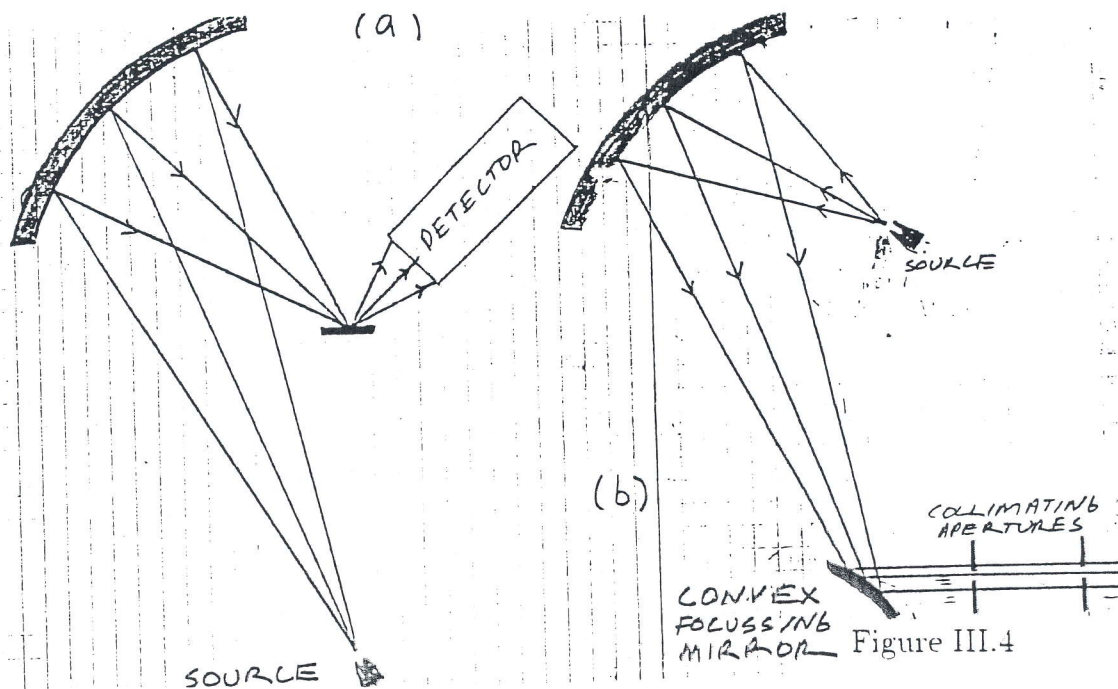
The simple beam enhancing configuration of figure (a) above, may not however be generally applicable to angularly resolved helium atom scattering experiments due to the degredation to momentum resolution resulting from the large transverse momentum spread in the focussed beam. If, however, it is possible to produce an atomic mirror of small radius of curvature i.e. if it is possible to form a reasonable quality reflecting metal surface on glass, (of no better quality than those produced presently by gold on mica), then a double reflection configuration as shown in figure (b) could concievably produce very intense parallel helium beams, the intensity improvement dependent upon the smallest radius of curvature possible for the convex focussing mirror.

All that needs to be attempted is to test a piece of highly polished glass coated with a metal overlayer in a helium scattering rig of good angular resolution to see if the elastic peak is noticably broadened by the presence of surface imperfections. If not, orders of magnitude gains in intensity would seem realistic expectations. How much one could increase the pressure in a He beam through such arrangements before intra-beam scattering becomes a problem, I have not yet researched in detail.

III.6   Testing of Mirror Accuracy

STM (or AFM) can be used to test the mirror surface (perhaps only in a limited way as indicated in section III.3) over small regions ($\simeq 1 \mu^2$). For testing the mirror form over large macroscopic areas, the laser interferometer presents itself as an ideal candidate. For example, the commercially available model MP2000 by Polytech is able to perform measurements over an area of 10×10 cm with a horizontal resolution of 1μ and a vertical resolution of $1.0 \AA$.

III.7 The Fresnel Zone Plate

For a number of reasons. the Fresnel zone plate apears presently as an excellent candidate for the focussing element of an imaging atom microscope. if the concomitant low count rate and resolution constraints imposed prove not too restrictive. The low count rate results from it's small acceptane solid angle. itself a consequence of a small physical size and macroscopically long focal length. The resolution constraint is imposed by the limits of modern technology to produce zone plates with finer free standing physical structures. Most attractive is the fact that high resolution micro zone plates already exists. whilst it is yet to be shown whether an atomic mirror capable of high resolution imaging is feasible on technological or even theoretical grounds. Pioneering work in the development of zone plates and their application to X-ray microscopy was made by the group of Schmahl at the University of Göttingen [6]. Recently. Carnal et al [4] used a high resolution micro zone plate ($\simeq .4\mu$) to image single and double slit structures with helium atoms as the imaging medium. Their results did not come close to realizing the theoretically predicted resolution limit of the zone plate itself. but this is explained by other resolution degrading factors inherent in their measurements. The characteristic form of the zone plate is illustrated in figure III.5 below.

The zone plate consists of alternating transmitting and opaque concentric rings with diameters increasing with the square root of the ring order n, the transmission function $t(\rho)$ being given by the expression:

$$t(\rho) = \begin{cases} 0. & \text{for } r_{2n} \leq \rho < r_{2n+1} \text{ (absorbing zone)}; \\ 1. & \text{for } r_{2n+1} \leq \rho < r_{2n+2} \text{ (transmitting zone)} \end{cases} \qquad (III.15)$$

where ρ is radial distance measured from the centre of the zone plate. $n = 0. 1. 2 ... n_{max} - 1$ with $2n_{max}$ being the number of zones. r_1 the innermost zone radius and the radii r_n related to r_1 through the expression:

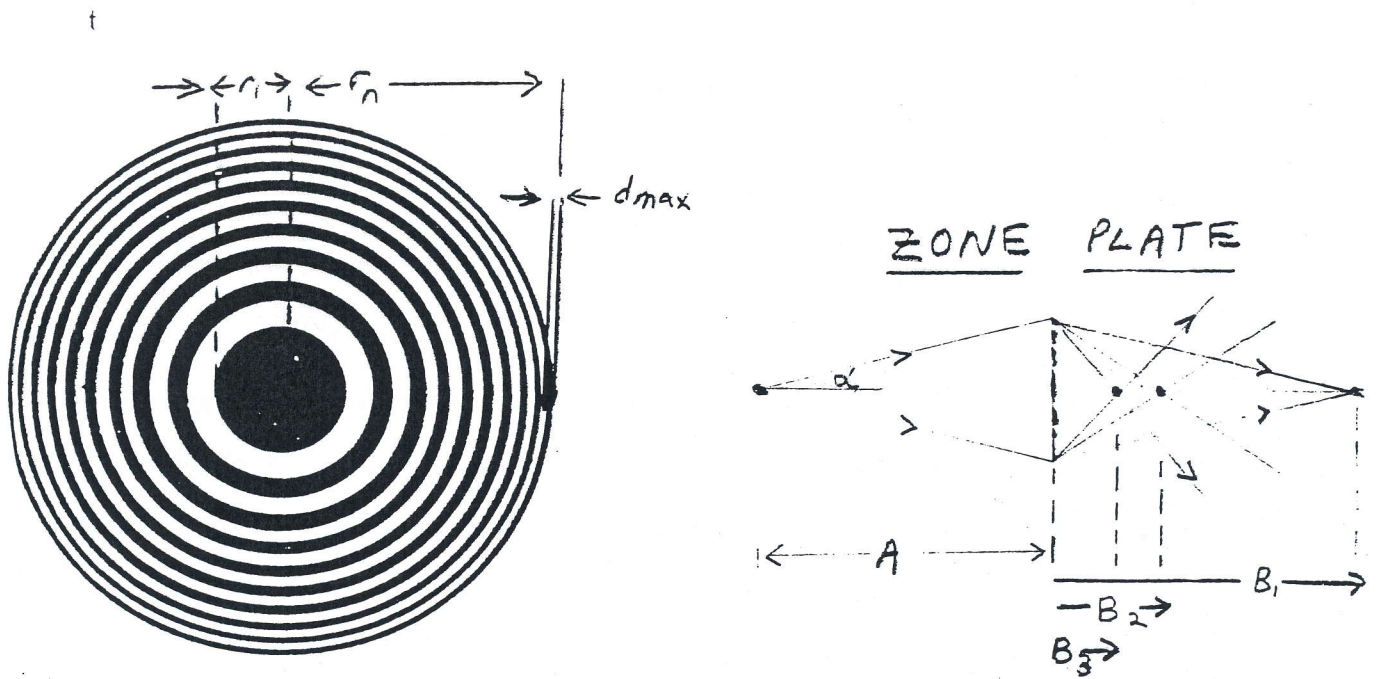$$r_n = \sqrt{n} \cdot r_1 \quad . \tag{III.16}$$

Figure III.5

The zone plate acts as a lens which images an object at a distance A onto images at distances B_m where A and B_m obey the lens equation:

$$\frac{1}{A} + \frac{1}{B_m} = \frac{1}{f_m} = \frac{m \lambda}{(r_1)^2} \tag{III.17}$$

Here m (integer) represents the order of diffraction. The relative flux o_m into the various orders m is given by the expression:

$$o_m = 1/m^2 \text{ for } m \neq 0 : \quad o_0 = (\pi/2)^2 . \tag{III.18}$$

Using the result that

$$\sum_{n=1}^{\infty} 1/n^2 = (\pi^2)/6 . \tag{III.19}$$

23

it is seen that the percentage of transmitted flux into the undiffracted zeroth order $m = 0$ component is 60 %. the percentage into the first order 24 %. into the second 6 % etc.

Compare the above formula with the mirror formula (III.7):

$$\frac{1}{D_{01}} + \frac{1}{D_{12}} = -\frac{2}{R} = \frac{1}{f}$$

where D_{01} and D_{12} are the object and image distances respectively. f is the focal length and R is the mirror radius. In contrast to the zone plate. no wavelength dependence of focal length is present. as Snell's law ($\theta_{incidence} = \theta_{reflected}$) is wavelength independent. The zone plate diffraction limited resolution δ_m is given approximately by the equation [4]:

$$\delta_m = \frac{1}{2\sqrt{2}n_{max}} \cdot \frac{r_1}{m} = \frac{d_{max}}{\sqrt{2}\,m} \qquad (III.20)$$

where d_{max} is the thickness of the outermost ring. Note that the zone plate resolution shows no explicit wavelength dependence. At first sight this appears in conflict with the Rayleigh criterion (III.13). The apparent parodox is however explained by rearranging equation ($III.20$) in the following way:

$$\delta_m = \frac{1}{2\sqrt{2}n_{max}} \cdot \frac{r_1}{m}$$

$$= \frac{r_1^2}{2\sqrt{2}r_{n_{max}} \cdot m} \qquad \text{(using } III.16\text{)}$$

$$= \frac{f_m \lambda}{2\sqrt{2}\,r_{n_{max}}} \qquad \text{(using } III.17\text{)}$$

$\lambda = 4\mathring{A}$ $d_{n_1} = 0.01 \text{Å}$

$v_{n-x} = 640\mu$ 24

$f = 8 cm$

$r_n = 6 M$

$n = 400$

$r_{n_{wa}} = 80 \mu$

$d_{nn} = 0.1 \mu$

$f = 8 cm$

$\lambda = 1 \mathring{A}$

$v = 3 m$

$r_n = \sqrt{n}\, r_1$

$d_{n_{cy}} = \frac{r_1}{2\sqrt{n}}$ $\sqrt{n} = \frac{r_1}{2 d_{nn}}$

$v_n = \sqrt{n}\, r_1$ $\Rightarrow n = r_1^2 / 4 d_{nn}^2$

$d_{max} = \frac{r_n}{2n}$

$r_n = d_{max} \cdot 2n$

$f_1 = \frac{r_1^2}{\lambda}$

$\lambda = 4\mathring{A}$

f_1

$8 \cdot 10^{-2} \times 16^{-10} = r_1^2$

$8 \cdot 10^{-12} = r_1^2$

$$= \frac{f_m \, \lambda}{4 \, \sin\alpha \, f_m} \qquad (\text{Figure } III.5)$$

$$= \frac{.25 \, \lambda}{\sin\alpha} \quad .$$

Except for a scaling factor, the result is identical to equation (III.13). The wavelength dependence of focal length for the zone plate means that any reduction in wavelength by a factor k is accompanied by a factor k increase in focal length. Thus, although the scattering angle for a given target spatial frequency has been reduced by a factor $1/k$ through reduction in wavelength, the acceptance cone of the zone plate has been decreased by a corresponding amount, thus the collected information and hence the diffraction limited resolution remains the same. Unlike the case of a focussing mirror where a wavelength dependence of resolution exists, we can here talk about the resolution of a given zone plate as an intrinsic property it possesses.

From equation (III.20) it is evident that resolution can be improved through the manufacture of a larger area zone plate by increasing n_{max}, through the production of a plate of smaller radius r_1, or by the selection of a higher order m image for imaging purposes. Let us first consider the relative merits of going along the first two paths.

The effect of doubling n_{max} is to produce a $\frac{1}{\sqrt{2}}$ reduction in ultimate resolution. The outermost zone element is at a radius $\sqrt{2}$ larger than before, it's thickness reduced by a factor of $\sqrt{2}$ and it's length $\sqrt{2}$ times longer. The focal length remains unchanged. Alternatively, scaling down the size of the plate by a factor $\sqrt{2}$ will also produce a $\sqrt{2}$ reduction in resolution, with all absorbing rings decreasing by a corresponding $\sqrt{2}$ factor in both thickness and circumference. The focal length is halved in this case. In both cases, the solid angle subtended at the target is doubled and the resolution determined by the thickness of the outermost ring (equation (III.20)). Therefore, from the perspective of improvement to resolution, the two approaches are of equal merit. The attractive aspect

25

of the latter is that the required apparatus size ($\propto$ focal length) scales down in proportion with the square of resolution and the mechanical stability is not degraded to the extent of the first method. Its relative disadvantage is the increased difficulty in handling and aligning a smaller focussing element. The production of a zone plate of finer structure is dependent upon the limits of technology and the intrinsic weakness of fine, self supporting structures.

The third avenue to improved spatial resolution is to select a higher diffraction order m for imaging, the resolution improving in direct proportion to m. Consider, for example, the feasibility of using the $m = 10$ focus with a zone plate such as that used by Carnal *et al* [4] to image the surface of a target (i.e. one with a central disc radius $r_1 = 9.38\,\mu$ and comprising of 64 rings). A field ionization detector will be used to detect the image. In this case, the theoretical resolution (as is the focal length) is ten times smaller than for the $m = 1$ order i.e. 400 Å !! However, there are significant problems to be surmounted. Firstly, the flux φ_m directed into this order is <u>100 times</u> smaller than for $m = 1$ and constitues only .2% of the total transmitted flux through the plate (eqns. (III.18), (III.19)). Thus count rate will be at a premium (see section IV). Secondly, the required beam monochromaticity, whose value is given approximately by the product $\sim n \cdot m$ [6], is now increased to 640. Finally and most seriously, it is a challenging task indeed to inhibit contributions from the other $m \neq 10$ diffraction orders from reaching the detector and thereby seriously degrading image contrast. Consider the figure below showing an ideal zone plate imaging a point source of atoms. Only rays corresponding to the $m = 8, 10, 12$ th orders are shown for clarity and an object magnification of $\simeq 1.0$ has been chosen.

Remembering that we can scan by moving the target rather than the detector, careful inspection of the above diagram reveals the existance of a disc of radius $\simeq \frac{r_1}{10}$ around the $m = 10$ focal point which is free of contributions from all other $m \neq 10$ orders. Therefore, if it were possible to focus the incident atom beam onto a circular area of the target surface

of radius $\leq \frac{r_1}{10}$ i.e. $\leq 1\,\mu$ in the present example. then contributions from the $m = 10$ order could be cleanly selected by a field ionization detector. Obviously. the stringency of the requirement imposed on the size of illuminated target area is somewhat relaxed if a lower $m < 10$ order is chosen for imaging purposes e.g. focussing to a spot of radius $\leq \frac{r_1}{2}$ ($\leq 5\mu$) is required if the $m = 1$ order is to be cleanly selected for imaging.
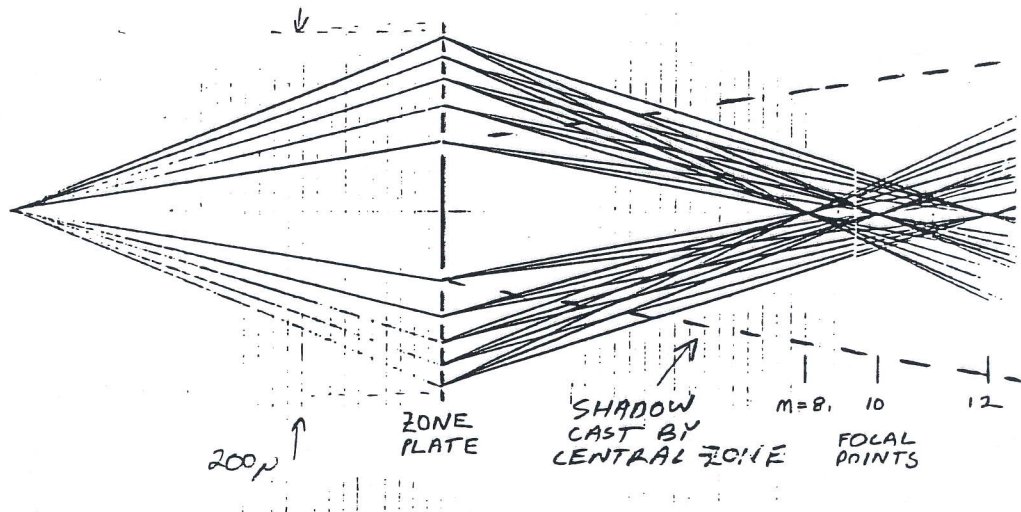

Figure III.6

This technique. of course. relies upon the highly stable alignment of all microscope components and a zone plate manufactured to considerable precision. Nevertheless. my aim has been to simply show that the use of a higher order image could be quite feasible if a "point like" field ionization detector is used. Note that because of the inverse dependance of focal length on diffraction order m. we could use a room temperature source to obtain the required high level of beam monochromaticity without fear that the apparatus length will prove too large. i.e. Use of the $m = 10$ order with a magnification of one and a room temperature atom source would result in a target to detector distance of 1.0 metre in the present example. not 10 metres as would be the case if the $m = 1$ order were used.

IV. Image Contrast

IV.1   Introduction

The very properties of chemical inertness and non-destructive interaction with surfaces. which so handsomely present helium as a candidate for a surface imaging medium. themselves greatly reduce the number of avenues available to obtain image contrast. Indeed. in the abscence of condensation. all areas of a surface will reflect atoms with 100 % probability. variations in scattered intensity through a given solid angle of observation (i.e. variations in the differential scattering cross section) providing the only means for image contrast. For this specific case of "diffraction contrast". it is interesting to note that the degree of contrast obtained is intimately related to the diffraction limited resolution of the imaging element itself. Imagine. for a moment. the effect of increasing the acceptane solid angle of the atom imaging element in a simple type B microscope (Figure 1). As the solid angle Ω tends towards 2π steradians. the diffraction limited resolution tends towards the limiting value of 0.61 λ [III.13]. but the measured variations in scattered atom flux between points on the surface tend towards zero. In other words. a perfect aberration free focussing element. collecting all scattered atoms from the surface under observation. would yield an image with no contrast at all !! It is only through imperfections in the imaging system. be they intrinsic or introduced. that information on surface structure is provided. Note that with other contrast methods (i.e. absorption contrast in a transmission electron microscope). resolution and contrast are not in any way in conflict with one another. This peculiar phenomenon only applies to diffraction contrast.

Before embarking upon upon a detailed discussion on contrast. I wish to consider first a few simple examples from optics which bring out clearly a number of pertinent concepts. It can be shown [7] that the far field diffraction pattern of a monochromatic wave passing through an aperture is simply the Fourier transform of the "aperture function". a function

28

which describes the field distribution across the aperture i.e. point to point variations in phase and amplitude. In the case of an incident plane wave, the aperture function is simply 1.0 i.e. constant in phase and amplitude over the entire aperture and zero outside. In this case the diffraction pattern is soley determined by the geometry of the aperture itself. For example, the intensity pattern $I(\theta)$ produced by a plane wave (wavevector $\underline{k}$) on a screen a distance D away after diffraction through a circular aperture of radius a is given by the well known result [7] :

$$I(\theta) \propto 2\left[\frac{J_1(ka\ sin\theta)}{ka\ sin\theta}\right]^2 . \qquad (IV.1)$$

the symmetry axis for θ being parallel to the direction of the incident wavevector. The smaller is the diffracting aperture, the larger the angular spread of the diffracted beam.

The situation changes entirely if the incident wavefront is not constant in phase or amplitude across the aperture. By choice of a suitable phase distribution, for example, one can arbtrarily rotate the symmetry axis of the diffraction pattern to any chosen direction (1-D example in ref. [7], pg. 335) or broaden it arbitrarily. Through such manipulation, a small aperture could be made to generate a narrower diffraction pattern than a larger aperture ! (Of course the minimum angular width in all cases is determined by the Rayleigh diffraction limit (III.13)). Thus diffraction through (or alternatively reflection from) large scale structures does not necessarily give rise to diffracted intensity into a small solid angle or directed along a fixed symmetry direction with respect to the incident beam. For this reason, when one considers the more complicated case of the scattering of a particle wave from a potential surface, caution must be applied when invoking the argument that "small scale structure diffract atoms through large angles whilst large scale structures leads to small angle scattering" due to the three dimensional nature of the scattering potential and the concomitant path length dependent phase variations it induces across the surface.

IV.2   Image Contrast Enhancement

I now wish to introduce the concept of contrast enhancement through filtering of the far field atom diffraction pattern before it's processing by an imaging lens. For illustration purposes. I consider the case of helium atom microscopy with a type B microscope configuration of a simple (rather unrealistic) surface consisting of small circular "atomic mirrors" (i.e crystallites), each of a different size and all perfectly oriented with respect to one another, superimposed upon an atomically rough background. Our interest will lie in resolving these small structures. Consider first the case of orientating the focussing element in the symmetry direction for elastic scattering from the tiny mirror surfaces as shown in the diagram.

Because the crystallite surfaces are flat, their aperture functions are constant and thus the argument that small crystallites (high spatial frequencies) leads to diffraction through large angles whilst large crystallites (low spatial frequencies) generate small angle diffraction patterns holds. the symmetry axis being the specular direction. Equation (IV.1) is applicable in this case. To illustrate the concepts of diffraction contrast. I have drawn a zone plate of 200 μ dimensions at a distance of .5 metres from the target surface under observation (the .4 μ resolution zone plate considered earlier). The angular distributions of diffracted atoms arising from "mirrors" of 4000 $\overset{\circ}{A}$. 8000 $\overset{\circ}{A}$ and 10μ in are illustrated. For structure of a given size to be resolved. the imaging lens must intercept at least half of the first order diffraction maxima [6]. To enhance image contrast. "spatial filtering" of the atom diffraction pattern can be performed i.e. one selectively prevents atoms scattered through a specific range of solid angles from ever reaching the detector. thereby giving contrast to certain length scales in the target.

Note that this filtering can be equally well performed at the entrance to the focussing element rather than at its back focal plane (the Fourier transform plane) where it strictly

should be performed. as the imaged target area is so small and the target to detector distance so large that the scattered atoms. before being processed by the lens. have already decomposed into the far field diffraction pattern of the surface.
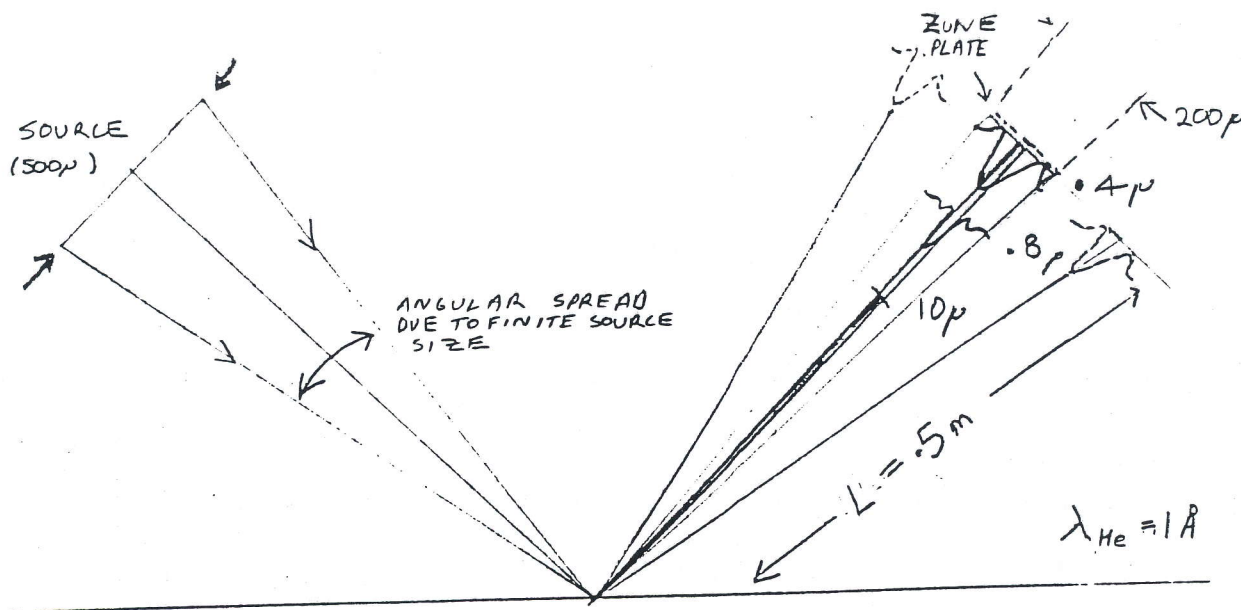

Figure IV.1

For an example. suppose one blocks out the central cone of atoms incident upon the zone plate corresponding in width to the principle maximum for crystallites of 8000 Å size. as indicated in the diagram. In this case. crystallites of between 4000 and 8000 Å in size are imaged with great contrast. whilst information concerning dimensions of greater than 8000 Å dimensions does not reach the detector. The diagram also shows how the effect of finite source size can completely disrupt this procedure of modifying the image contrast and/or countrate. by smearing out the diffraction patterns. if the size range of interest on the target surface is rather large (diffraction through small angles) or the focussing element subtends a small solid angle with respect to the target i.e. has poor diffraction limited resolution. For the particular imaging element considered in the diagram (a 200 μ zone plate). it is evident that an effective source size of the order of 50μ is required to obtain good control over diffraction contrast through filtering and to maintain countrate

31

by intercepting a large proportion of the diffracted current ! Countrate and control over contrast are equally sensitive to any spread in orientation between the crystallites (mosaic structure) which may be present.

IV.3 Contrast fom Elastic Scattering

I wish now to consider the specific case of scattering from a crystal surface. where one is primarily interested in the defects i.e. step edges. adatoms. mosaic structure etc. rather than the intervening ordered regions of surface. It is then important to have some idea of the angular distribution of scattered particles from the particular defect species of interest in order to be able to estimate how much of the scattered signal will be intercepted by the finite sized imaging element employed. More specifically. if all angular distributions of interest turn out to to be diffuse. then the zone plate might be ruled out as an imaging element purely upon count rate (sensitivity) considerations. For example. with an atom source of intensity 10^{20} counts/steradian/sec at a distance of .25 metres from the target and a 4000 $\overset{\circ}{A}$ resolution zone plate as previously considered ($m = 1$ focus and magnification 1.0). an isotropic distribution of scattered atoms from a 4000 $\overset{\circ}{A}$ defect would result in a count rate of only 0.15 Hz. the zone plate subtending only 3.9 $\times 10^{-8}$ sr at the target ! Of course. no scattering is truly isotropic. but remembering that the zone plate considered in this example subtends an angle of only .01 degrees at the target. then <u>any</u> scattering falling outside of the collection cone could well be defined as diffuse. For example. in the calculations by Drolshagen and Vollmer [10]. scattered intensity from the isolated atomic defects considered was largely concentrated into a $4°$ cone i.e. into 1.6×10^4 times the solid angle subtended by the zone plate itself. In such a case. an alternative contast technique to be decribed may provide the solution to low count rate.

Suppose. for the sake of argument. we are observing with a zone plate a surface under plane wave illumination. Consider scattering from a weak isotropic scatterer. dimensioned

32

as the size of the instrumental resolution δ. on an otherwise perfect crystal substrate (figure below). I define the reflected intensity from an observed region far from the defect as I_{refl}. Higher order m $\neq$ 0 elastic scattering and inelastic scattering processes are disregarded in this simple model.

POSITION A
OBSERVATION OF
DIFFUSE SCATTERING

POSITION B
OBSERVATION O
ELASTIC SCATTER

Specular

ISOTROPIC
SCATTERING FROM
DEFECT

SAMPLE
SCANNED ACROSS
VIEWCONE OF
LENS

δ

POSITION A

COUNTRATE

$6.4 \times 10^{-9} I_{DEF}$

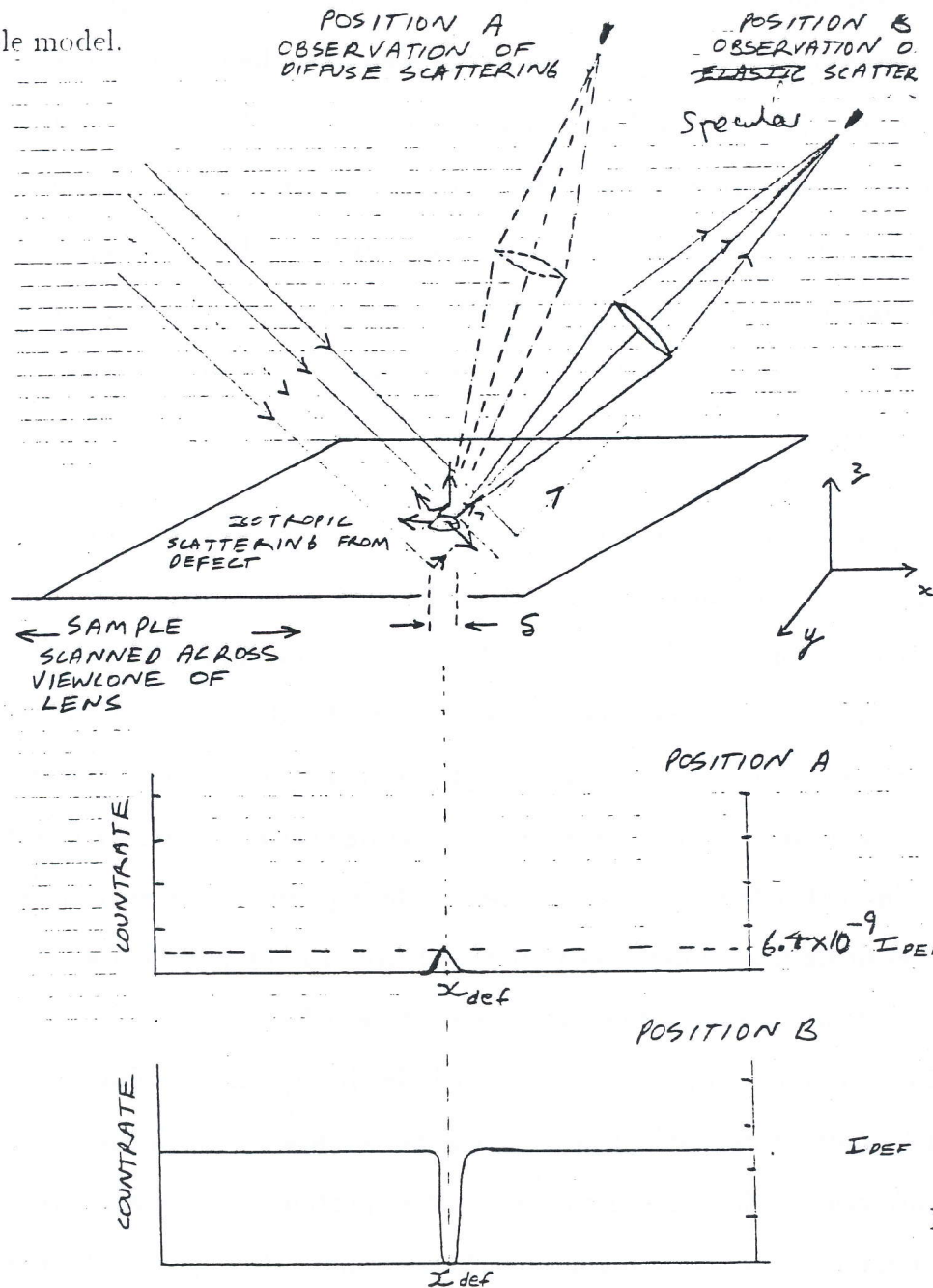X_{def}

POSITION B

COUNTRATE

I_{DEF}

X_{def}

Figure IV.2

The atom diffraction pattern consists of the weak isotropic component from the defect and the intense directed signal resulting from the flat crystal substrate. Let us first consider the situation when the detector is oriented in an arbitrary direction <u>other</u> than in

33

the direction of the elastically scattered specular beam. (e.g. position A in diagram). As the defect is scanned over, the countrate rises from zero to a maximum value of $6.2 \times 10^{-9} I_{ref}$ at position x_{def} and then back again to zero. Now consider the complementary approach. What happens to the elastic countrate as we scan over the defect ? The count rate falls from a value of I_{ref} to $6.4 \times 10^{-9} I_{ref}$ at x_{def} and then rises back again to its original value, the count rate (sensitivity to the defect) has been increased by a factor of 1.6×10^8 !! The improvement in sensitivity has been achieved through measuring the loss of elastic signal through diffuse scattering, regardless of into which solid angle the diffusely scattered particles are directed i.e. in this mode we integrate over all directions for the diffusely scattered particles.

This was, of course, an extreme example chosen explicitly to illustrate that potentially large gains in count rate are available through such a procedure. Furthermore, the enhancement technique is clearly not applicable to the imaging of any arbitrary target surface, but only to those possessing large areas of well ordered crystal. Note that although in this count rate enhancing technique, information concerning the exact form of defect scattering potentials is lost in the act of integrating over all scattering directions, contrast between different defect types is still present through their differences in scattering cross sections resulting from differences in physical size. In any practical application however, the degree of dip in elastic intensity observed as defect structure is scanned would depend upon a number of factors. These include the imaging resolution δ relative to the size of defect structures being observed, the percentage of the elastic intensity going into higher diffraction orders and of course, most importantly, the exact form of the angular distribution for elastic scattering from each particular defect species observed. Finally, the technique is extremely sensitive to the effects of finite source size, focussing of the incident beam and mosaic spread in the target (section IV.3), which all conspire to smear out the diffraction pattern of diffracted atoms.

V. Conclusion

My goal over the past five months has been to gain an overview of the field of atom optics and to establish, where possible, optimum design parameters for an atom microscope. As the design of an atom microscope requires knowledge in such a broad and diverse range of specialist areas, I have only had time to touch upon the surface of many crucial to the realization of a working instrument. Nevertheless, from the present perspective, the following does appear true:

(a) That the best chance of developing a helium atom microscope of resolution ≤ 1000 Å lies in selecting a higher order image produced by a Fresnel zone plate with "point like" field ionization detector. Significant enhancement of incident beam intensity, best rendered through the agency of an atomic mirror, a second zone plate or a combination of zone plate and mirror is required to increase countrate levels. Furthermore, the primary beam must be focussed to a spot size of $\simeq 1 \rightarrow 5 \mu$ to eliminate the effect of overlapping images at the detector plane.

(b) Although of use as a means to enhance incident beam intensity, the resolution degrading effects of mosaic structure and the extreme accuracy of form required on the macroscopic scale dismiss the atomic mirror as a candidate for a ≤ 1000 Å microscope imaging element. Nevertheless, the development of the "best atomic mirrors in the world" is an attractive goal in itself, given the wide application in beam experiments high quality atomic mirrors would undoubtedly receive.
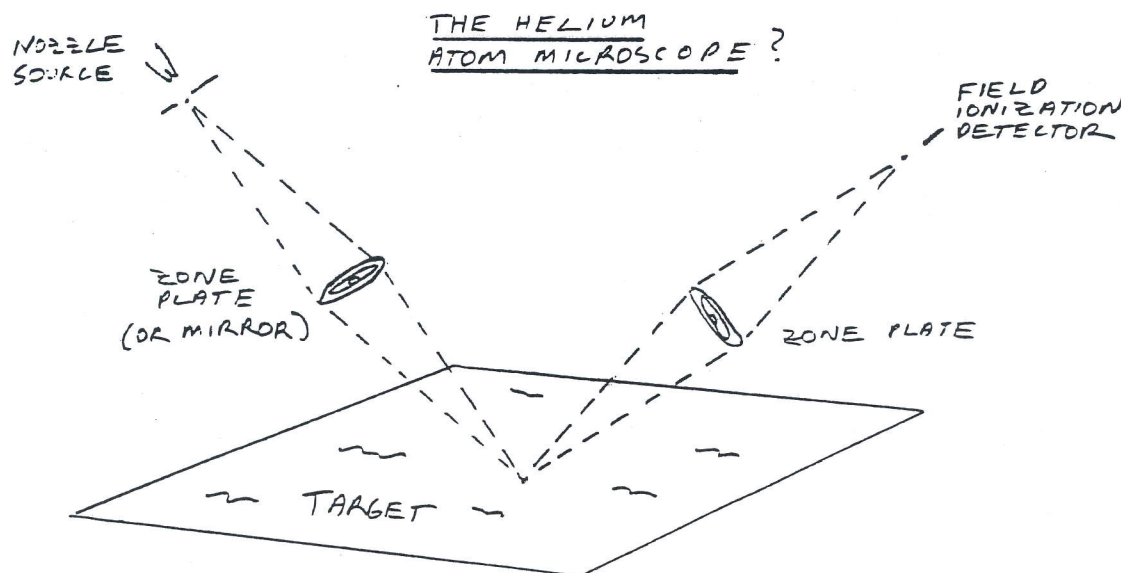
In the light of these conclusions, the following course of action presents itself:

(i) To establish with certainty, through discussions with people at the forefront of zone plate research, what are the highest resolution zone plates which can be presently produced and the prognosis for their future improvement (e.g. Find out what are the technological limits to producing zone plates of finer structure. Does the decreased structural integrity of

ever finer free standing structures already limit further improvements ?). The procurement of such a device for incorporation into a prototype microscope. Investigation into the possibility of constructing a reflecting zone plate, promising perhaps improved resolution and count rate due to a finer achievable ring structure.

(*ii*) To test, in a helium scattering apparatus, the quality of various metal surfaces deposited on a highly polished glass substrates, with the view of developing high quality atom mirrors for primary beam intensification purposes.

In summary, from the perspective of resolution, count rate and contrast, a ≤ 1000 Å atom microscope appears already feasible with present levels of technology. A possible configuration is shown in the diagram below. Clearly, much detailed planning and laboratory based investigations will be required to achieve it's realization.

THE HELIUM
ATOM MICROSCOPE ?

NOZZLE SOURCE

FIELD IONIZATION DETECTOR

ZONE PLATE (OR MIRROR)

ZONE PLATE

TARGET

36

VI. Appendix I

Consider first the equation of the ideal elliptical focussing mirror. Taking the origin at $(a, 0)$ as indicated in figure 3.1. the ellipse is described by the following formula:

$$\frac{(x_\epsilon - a)^2}{a^2} = 1 - \frac{y^2}{b^2} \qquad (III.1)$$

where

$$a = \frac{D_{01} + D_{12}}{2} \quad \text{and} \quad b^2 = D_{01}D_{12} \quad [8] . \qquad (III.2)$$

After some rearrangement. (3.1) becomes:

$$x_\epsilon = \frac{D_{01} + D_{12}}{2} \left(\frac{y^2}{2D_{01}D_{12}} + \frac{y^4}{8(D_{01}D_{12})^2} + \ldots \right). \qquad (III.3)$$

using the expansion

$$\sqrt{1 + x} = 1 + \frac{x}{2} - \frac{x^2}{8} + \ldots \quad . \qquad (III.4)$$

The equation of a circle. radius R and origin at $(R, 0)$. is given by the expression:

$$(x_c - R)^2 + y^2 = R^2 \quad . \qquad (III.5)$$

Rearranging and using expansion $(III.4)$ as before. this becomes:

$$x_c = \frac{y^2}{2R} + \frac{y^4}{8R^3} + \ldots \quad . \qquad (III.6)$$

37

<u>If</u> the circle radius is chosen such that :

$$\frac{1}{D_{01}} + \frac{1}{D_{12}} = -\frac{2}{R} \qquad \text{The mirror formula} \qquad (III.7)$$

then the equations for the ellipse and circle are equal to first order. Substituting equation (III.7) into (III.3) we can rewrite the equation of the ellipse in terms of the radius R of the circle which best approximates it's shape in the following way.

$$x_\epsilon = \frac{y^2}{2R} + \frac{y^4}{8(D_{01}D_{12})R} + \dots \qquad (III.8)$$

The parabolic approximation to the ellipse is simply the first term in the above series:

$$x_p = \frac{y^2}{2R} \qquad (III.9)$$

In summary, we have:

$$x_c = \frac{y^2}{2R} + \frac{y^4}{8R^3} + \dots \qquad : circle$$

$$x_\epsilon = \frac{y^2}{2R} + \frac{y^4}{8RD_{01}D_{12}} + \dots \qquad : ellipse$$

$$x_p = \frac{y^2}{2R} \qquad : parabola$$

The error (aberration) in arrival position δ_y of a ray (particle) on the distant focal plane Σ_F perpendicular to and passing through D_{12}, is given by the product of the mirror

38

to screen distance D_{12} and the difference in slope of the circular and parabolic surfaces respectively from the ideal elliptical form :

$$\delta y_c = (\frac{dx_c}{dy} - \frac{dx_\epsilon}{dy}) D_{12} = \frac{y^3}{2R} (\frac{D_{12}}{R^2} - \frac{1}{D_{01}}) \qquad (III.10)$$

$$\delta y_p = (\frac{dx_p}{dy} - \frac{dx_\epsilon}{dy}) D_{12} = \frac{y^3}{2RD_{01}} \qquad (III.11)$$

The difference in height between the circular and parabolic surfaces respectively and the ellipse which they approximate is given by the following two equations:

$$x_{c\epsilon} = x_c - x_\epsilon = \frac{y^4}{8R} (\frac{1}{R^2} - \frac{1}{D_{01}D_{12}}) \qquad (3.11)$$

$$x_{p\epsilon} = x_p - x_\epsilon = -(\frac{y^4}{8RD_{01}D_{12}}) \qquad (III.12)$$

VII. References

[1] R. B. Doak. "Focussing of an Atomic Beam", submitted for publication (1990).

[2] T. Sakurai, A. Sakai and H. Pickering. "Atom-Probe Field Ion Microscopy and its Applications", Advances in Electronics and Electron Physics, Supplement **20** (1989).

[3] C. E. D. Chidsey, D. N. Loiacono, T. Sleator and S. Nakahara. "STM Study of the Surface Morphology of Gold on Mica", Surface Sci. **200** (1988) 45.

[4] O. Carnal, M. Sigel, T. Sleator, H. Takuma and J. Mlynek, "Imaging and Focussing of Atoms by a Fresnel Zone Plate", submitted for publication (1991).

[5] R. D. Heidenreich. "Fundamentals of Transmission Electron Microscopy", Vol. XIII, Interscience Monographs and Texts in Physics and Astronomy, Editor R. E. Marshak, Wiley (1964).

[6] G. Schmahl, D. Rudolph, P. Guttmann and O. Christ, "Zone Plates for X-Ray Microscopy", Spinger Series in Optical Sciences Vol. **43**, Editors G. Schmahl and D. Rudolph (1984) 63.

[7] E. Hecht and A. Zajac. "Optics", Addison-Wesley Publishing Company Inc., (1974) pgs. 176, 335.

[8] M. V. Klein. "Optics", John Wiley and Sons Inc., (1970).

[9] L. D. Landau and E. M. Lifshitz. "Theory of Elasticity", Pergamon Press Ltd., (1970) pg. 51.

[10] G. Drolshagen and R. Vollmer. J. Chem. Phys. **87** (1987) 4948.